

Double Patterning Technique Using an Aluminum Hardmask

Brian Lindenau

Abstract—The goal of this project was to successfully demonstrate a double patterning technique using equipment available at the SMFL at RIT. Traditional methods of increasing resolution have been essentially exhausted; therefore new methods of increasing resolution are needed. One of these new methods is double patterning, which splits a dense pattern into two less dense patterns which are imaged in two steps, thereby reducing imaging constraints. Overall a proof of concept of the double patterning process was achieved. Imaging of 0.5 μm drawn features was demonstrated, resulting in 0.3 μm post-etch.

Index Terms—double patterning, hardmask, BARC

I. INTRODUCTION

Increasing resolution in a lithographic system has been a constant goal in the semiconductor industry. Feature sizes have continued to shrink, forcing lithographic systems to adapt. Minimum resolution is determined by the Raleigh Criterion. The traditional methods of increasing resolution have been to decrease the wavelength of the radiation used, thereby creating smaller diffraction angles, or to increase the NA of the system, thereby capturing larger diffraction angles. These traditional methods of increasing resolution are approaching their limit. Reducing wavelength below 193nm to 157nm has proven to be extremely problematic. The traditional fused silica lenses used in modern lithography equipment are highly absorptive at this smaller wavelength. Also, resist systems for 157nm have yet to be developed.

Increasing NA has shown more promise, but is still approaching a limit. Increasing NA past 1 has now been made possible due to immersion systems, which is essential for future minimum feature sizes. However, these systems are new and most likely will introduce new problems. A problem that has already arisen is finding a high-index immersion liquid other than water, to boost NA even further. Also, there is a practical limit on how high the index of the immersion fluid can be, as the fluid index cannot exceed the index of the photoresist, which is typically around 1.6-1.7.

These issues with traditional methods of increasing resolution have lead to other less desirable, but possible solutions. One of these methods includes double patterning. Double patterning utilizes the relationship between duty-ratios and resolution. Imaging smaller features becomes much easier when the duty ratios are large. Unfortunately, densely packed features are still required in chip designs. Double

patterning allows for higher duty-ratios and still results in densely packed features. This is accomplished by splitting densely packed features with duty-ratios near 1:1 into two different mask sets, with duty ratios of 1:3. The wafers are then exposed and patterned twice, the first pattern of 1:3 features, followed by the second pattern of 1:3 features, which are placed in between the first set of features. This creates a set of densely packed features, without having to image them all at the same time, thereby effectively increasing the resolution of the system. This can be proven by utilizing Eq. 1, known as the Rayleigh Criterion. Essentially, this technique allows for k_1 values less than 0.25.

$$hp_{\min} = \frac{k_1 \lambda}{NA} \quad (1)$$

Currently, there are many different double patterning techniques, and they are generally divided into two separate categories: processes using a single etch step, and processes using two etch steps. The latter technique was used in this experiment.

The target layer for the double patterning process is the polysilicon gate layer. This layer typically has the smallest and most critical features in a CMOS process. The process uses a single hardmask of aluminum, in which the first pass pattern is transferred. Aluminum was selected for the hardmask material for several reasons. Aluminum has been a common material in semiconductor manufacturing, and deposition and etching techniques are well developed and characterized. Also, from MEMS applications, aluminum is known to have high selectivity in common silicon etch chemistries (~300:1). However, using aluminum has significant challenges. The reflectivity of the material created the first challenge that needed to be addressed, due to the standing wave effects and resist thickness sensitivity it created. A bottom anti-reflective coating (BARC) from Brewer Science, Inc. was utilized to mitigate this issue. Another challenge arose from the fact that aluminum etch processes typically have not been developed for the critical feature sizes needed for the gate layer.

II. PROCEDURE

The general process flow is illustrated in Fig. 1. The process begins with the film stack for the polysilicon gate layer. From here, a thin layer of aluminum is deposited (1000 Å). The first pass lithography is then performed, and the resulting pattern is transferred to the underlying aluminum layer. After the aluminum is etched and the resist is removed, the second pass lithography is performed. Finally, both passes are etched into the underlying polysilicon layer to achieve the final pattern. The photoresist and aluminum are then stripped from the wafer, leaving only the poly pattern. For a detailed process flow please see the attached table.

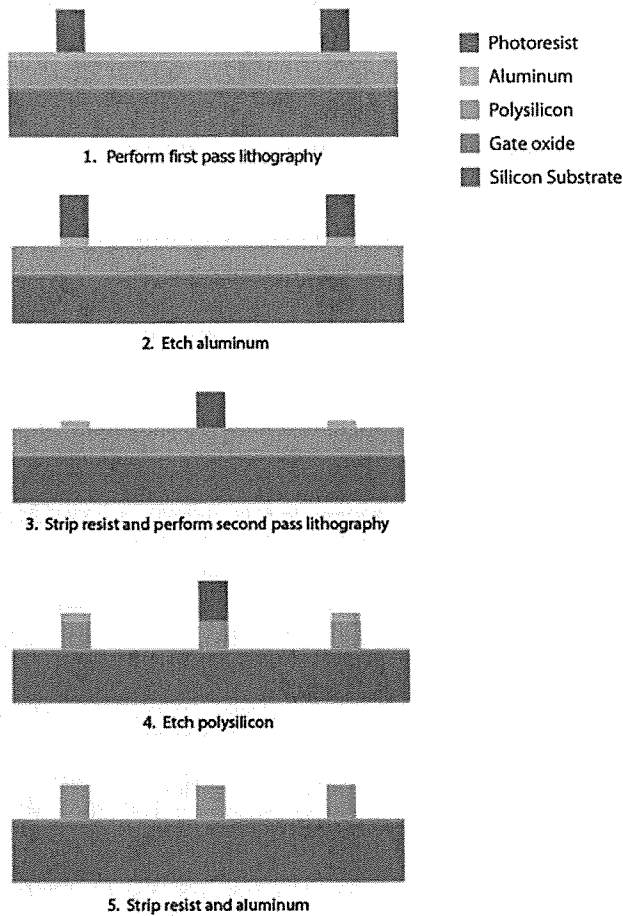


Figure 1: General process flow for double patterning technique

III. RESULTS

A. BARC simulation

A BARC from Brewer Science (i-CON 16) was utilized for this process. The performance of the BARC was simulated using *Prolith* lithography simulation software. A basic swing curve (resist thickness v. reflectivity) was created for two scenarios: with and without 1600 Å of BARC. These simulations were completed for both passes of lithography, since both passes have reflective substrates. The results of these simulations are shown in Figs. 2 and 3. The purple

lines are for no BARC, and the green lines are with the BARC. The results show a significant improvement in reflectivity in both cases. The amplitude of the swing curve for the first pass was reduced from 0.34 to 0.01, and the amplitude for the second pass was reduced significantly as well.

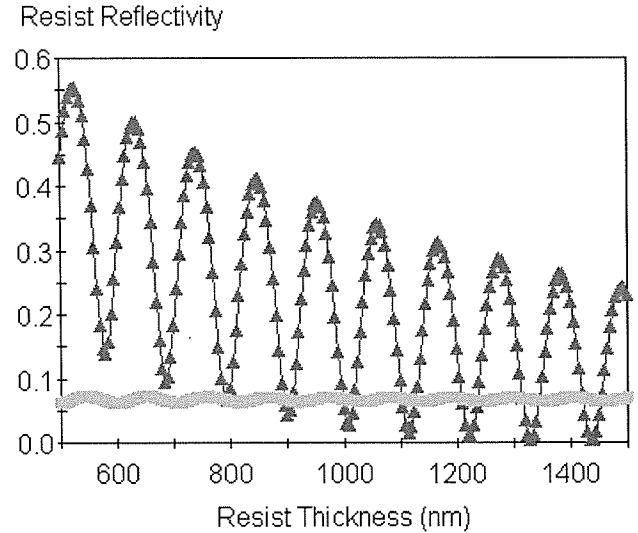


Figure 2: Swing curve simulation results for first pass (aluminum)

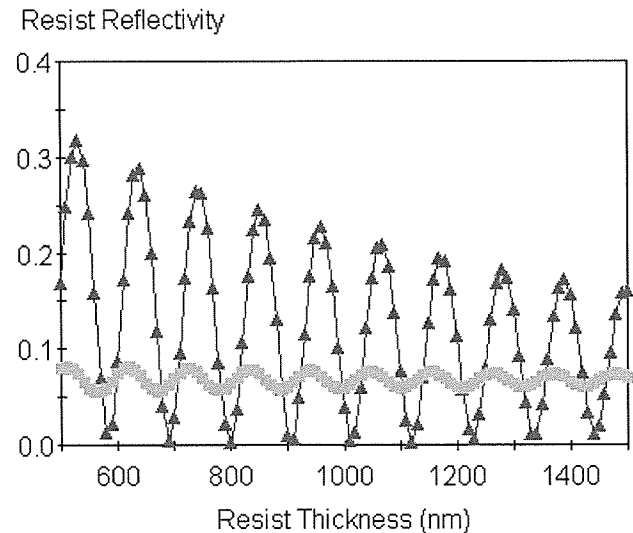


Figure 3: Swing curve simulation results for second pass (poly)

B. First Pass Lithography

Imaging of 0.3 μm drawn features was achieved in the first lithography step, as well as 0.5 and 1 μm drawn features. An optical image of the results is shown in Fig. 4. The primary challenge in this step was achieving the correct focus and exposure settings for the imaging step. This was done using focus/exposure arrays, which were qualitatively evaluated. The optimum settings were found to be a dose of 320 mJ, and a focus setting of +0.2 μm .

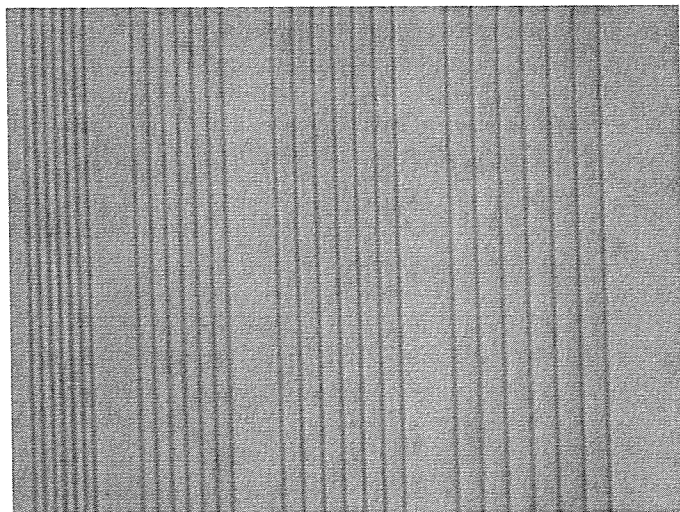


Figure 4: Optical image of $0.3\ \mu\text{m}$ drawn lines after first pass lithography

C. BARC etch

The BARC used in this process was not wet-developable, therefore an etch process was developed to etch the thin BARC layer before attempting the aluminum etch. This etch was performed in the LAM 490, using a chemistry of 10 sccm of O_2 , and 100 sccm of SF_6 . The etch rate was found to be $\sim 50\ \text{\AA}/\text{sec}$, with minimal resist erosion.

D. Aluminum etch

The aluminum etch for this process was adapted from an existing aluminum etch recipe meant for much thicker films ($\sim 0.75\ \mu\text{m}$). The etch rate proved to be extremely slow for the first several attempts for an unknown reason. One possibility was an increase in the thickness of the native aluminum oxide “skin” on the surface of the aluminum film, which may have been caused by exposing the aluminum surface to an oxygen ambient during the BARC etch. Another possible cause in the differing results for the thinner film could be an unknown acceleration of the etch rate during the etch process. This effect was finally compensated for by increasing the time of the first stage of the etch, which is the portion of the etch recipe meant to break through the aluminum oxide skin. Also, the etch time for the second stage of the etch was also significantly increased. This resulted in a complete aluminum etch. The $0.3\ \mu\text{m}$ drawn lines were still intact after the aluminum etch. An optical image of the aluminum lines post-etch and after resist strip is shown in Fig. 5.

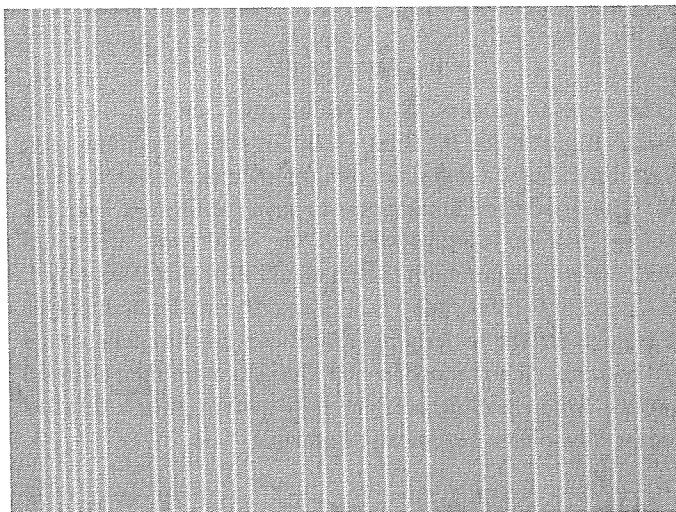


Figure 5: Optical image of pattern after aluminum etch

E. Second Pass Lithography

Optimal imaging settings were found using the same approach as the first pass, which used focus/exposure arrays and a qualitative assessment. The imaging of the $0.3\ \mu\text{m}$ drawn lines was not achieved during the second pass. Possible reasons for this include optical proximity interactions with the aluminum lines in between the imaged features, topography issues, and BARC dishing in between the aluminum lines. Future process optimizations may or may not improve imaging capabilities of this step. An optical image of the $0.5\ \mu\text{m}$ drawn lines are shown in Fig. 6.

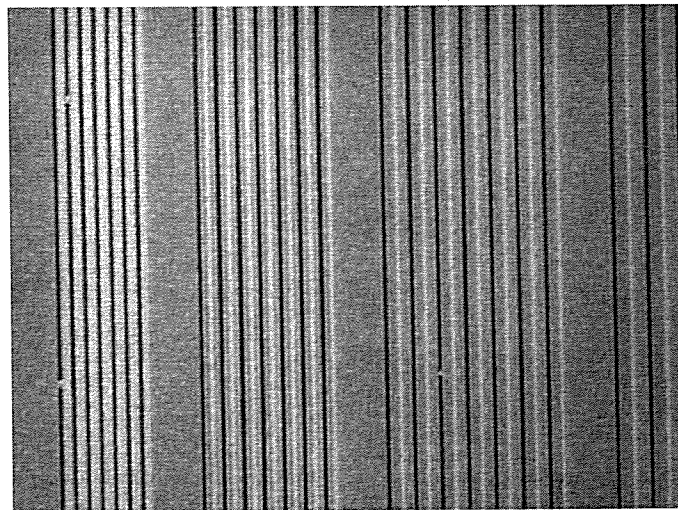


Figure 6: Optical image of second pass imaging results, where the dark lines are photoresist, and the light lines are aluminum features.

The primary concern in the second pass lithography step was overlay; however, this proved to be the parameter that gave the least amount of difficulty. The results of the overlay errors were immeasurably small using $0.1\ \mu\text{m}$ verniers. A high-magnification image of these alignment verniers is shown in Fig. 7.

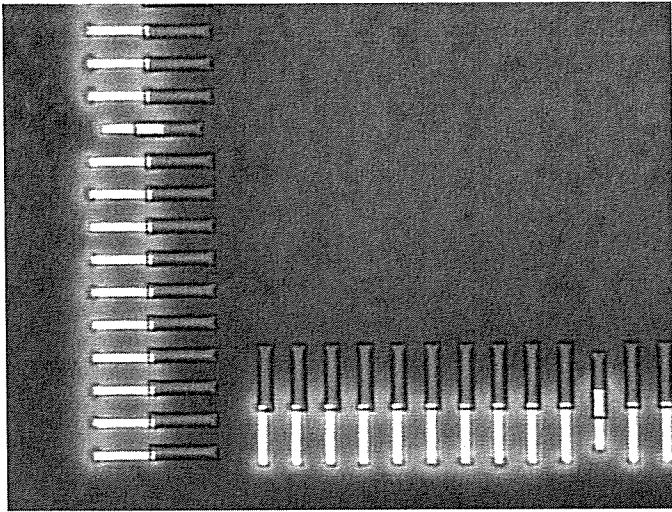


Figure 7: High-magnification image of 0.1 μm verniers, showing little to no overlay error.

F. Polysilicon etch

The polysilicon etch proved to be the most difficult part of the process. The etch was first attempted on the LAM 490, using an existing recipe intended for etching a 4000 Å poly film, which was the thickness of the poly used in this experiment. The results of this etch showed complete hardmask erosion, as well as resist undercutting for all feature sizes below 1 μm . The use of the LAM 490 for this etch was abandoned.

The Drytek Quad RIE system was utilized instead, as well as a poly etch recipe already adapted for a RIT factory process. The results of this etch was mixed. Most patterns showed signs of hardmask lifting, and some erosion. An example of this lifting is shown in Fig. 8. All 0.3 μm drawn patterns were completely eroded, and most 0.5 μm features were successfully transferred from the second pass imaging, however the hardmask for these patterns were shifted or completely lifted. Both passes of some 0.5 μm patterns were transferred intact. An example of these patterns is shown in Fig. 9.

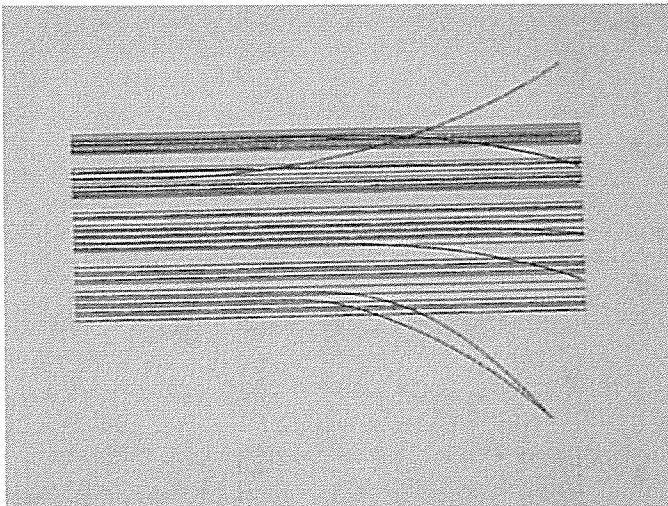


Figure 8: Optical image showing hardmask lifting after poly etch

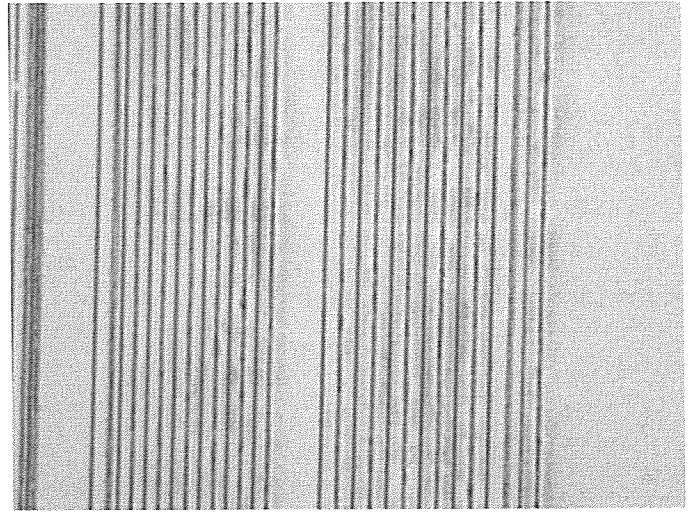


Figure 9: Optical image of final pattern transfer, after resist strip and aluminum strip. Evidence of shifted features is present.

G. SEM images

The pattern shown in Fig. 9 was also observed using a SEM, and is shown in Figs. 10 and 11. The images show that the 0.5 μm drawn lines became 0.3 μm poly lines after etch. The images also show a significant feature integrity difference between the lines protected with photoresist, and those protected by the aluminum hardmask. The hardmask-protected features show some damage and line edge roughness. In Fig. 11, the evidence of shifting hardmask features is clearly seen. Also, the CD error from pass-to-pass appears to be very minimal.

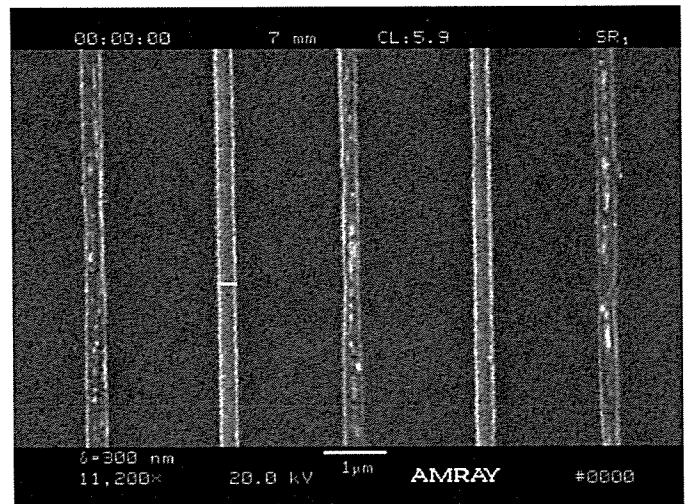


Figure 10: SEM image of 1:3 pitch, 0.5 μm drawn features, showing a CD post-etch of 0.3 μm

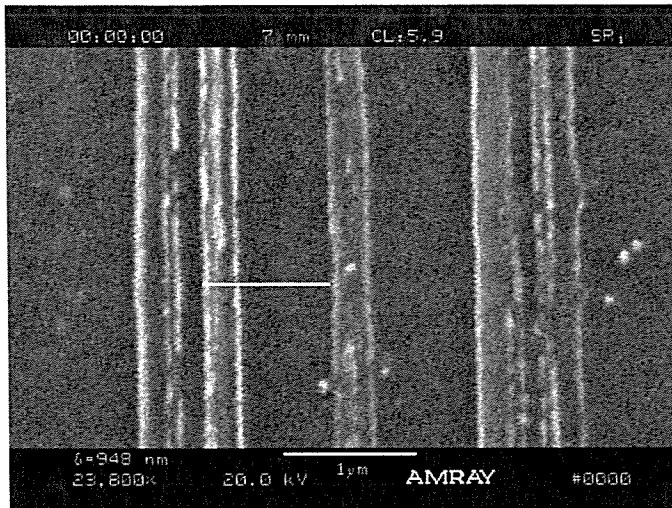


Figure 11: SEM image of 1:1 pitch, 0.5 μm drawn features. The image shows significant feature shifting.

IV. CONCLUSION

Overall, a proof of concept of a double patterning process using aluminum as a hard mask was achieved. Imaging of 0.5 μm drawn features was achieved with little to no overlay error, with a final CD after etch of 0.3 μm . Significant improvements can still be made to this process, specifically in the etch steps. The results show that a double patterning process is achievable at RIT.

REFERENCES

- [1] Stephen D. Hsu, et al., "Double Exposure Techniques for 45nm Node and Beyond", SPIE BACUS Vol. 5992, pp. 557-572, 2005
- [2] C. Linder, et al., "Deep Dry Etching as a New IC Compatible Tool for Silicon Micromachining," *Proc. Transducers '91, the 6th International Conference on Solid-State Sensors and Actuators Digest of Technical Papers*. San Francisco, CA: IEEE Press, June 24-27, 1991, pp. 524-527

Step	Action	Tool	Process details
1	Deposit aluminum	CVC 601	1000 W 450 secs 5 mT Target thickness: 1000 Å
2	Spin on BARC	CEE Hand Coater	2500 rpm 60 sec
3	Post-application bake	Hotplate	180 60 sec
4	Coat with resist	SSI Track	Recipe: coat 10000 Å thickness
5	Expose 1st pass	Canon Stepper	Recipe: arandall_nwell 320 mJ +0.2 µm
6	Develop	SSI Track	Recipe: develop
7	Etch BARC	LAM 490	Recipe: ash 35 secs 325 mT 140 W 10 sccm O ₂ 100 sccm SF ₆
8	Etch aluminum	LAM 4600	Stage 1: 15 secs 250 W 25 sccm N ₂ 100 sccm BCl ₃ 10 sccm Cl ₂ 15 sccm CF ₄ Stage 2: 70 secs 125 W 40 sccm N ₂ 50 sccm BCl ₃ 60 sccm Cl ₂ 15 sccm CF ₄ Stage 3: 10 secs 125 W 50 sccm N ₂ 50 sccm BCl ₃ 45 sccm Cl ₂ 15 sccm CF ₄
9	SRD	SRD	-
10	Ash resist/BARC	Branson Asher	Recipe: hardash
11	Spin on BARC	CEE Hand Coater	2500 rpm 60 sec
12	Post-application bake	Hotplate	180 60 sec
13	Coat with resist	SSI Track	Recipe: coat 10000 Å thickness
14	Expose 2nd pass	Canon Stepper	Recipe: arandall_align 300 mJ +0.2 µm
15	Develop	SSI Track	Recipe: develop
16	Etch BARC	LAM 490	Recipe: ash 35 secs 325 mT 140 W 10 sccm O ₂ 100 sccm SF ₆
17	Etch Poly	Drytek Quad	Recipe: facpoly 225 secs 190 W 40 mT 30 sccm SF ₆ 10 sccm CHF ₃
18	Ash resist/BARC	Branson Asher	Recipe: hardash
19	Strip aluminum	Aluminum etch	30 secs, or until visibly removed
20	SRD	SRD	-